# The Sommerfeld precursor in photonic crystals

Uitham, R; Hoenders, BJ

*Published in:*
Optics Communications

*DOI:*
10.1016/j.optcom.2005.12.077



*Publication date:*
2006

Available online at www.sciencedirect.com
SCIENCE DIRECT®
Optics Communications 262 (2006) 211–219
OPTICS COMMUNICATIONS
www.elsevier.com/locate/optcom

# The Sommerfeld precursor in photonic crystals

R. Uitham *, B.J. Hoenders

*University of Groningen, Institute for Theoretical Physics and Materials Science Center, Nijenborgh 4, NL-9747 AG Groningen, The Netherlands*

Received 28 September 2005; received in revised form 9 December 2005; accepted 28 December 2005

**Abstract**

We calculate the Sommerfeld precursor that results after transmission of a generic electromagnetic plane wave pulse with transverse electric polarization, through a one-dimensional rectangular $N$-layer photonic crystal with two slabs per layer. The shape of this precursor equals the shape of the precursor that would result from transmission through a homogeneous medium. However, amplitude and period of the precursor are now influenced by the spatial average of the plasma frequency squared instead of the plasma frequency squared for the homogeneous case.


*PACS:* 42.25.Bs; 42.70.Qs; 78.20.Ci

*Keywords:* Photonic crystal; Sommerfeld precursor; Pulse propagation

## 1. Introduction

The propagation of electromagnetic pulses in photonic crystals [1] exhibits many interesting phenomena. Most familiar is the photonic band-gap. This effect allows photonic crystals to be applied in for instance information technology as small-scale and low-loss wave-guides [1], or in fundamental research as devices that control spontaneous atomic photon emission [2]. Another interesting effect of a photonic crystal is that it can reduce the magnitude of the group velocity of an electromagnetic pulse considerably [3]. Theory predicts that this group speed can approach zero in photonic structures with many periods [4]. This allows for applications of photonic crystals as optical delay lines or as data storage compounds [5]. Not only small group velocities have been observed in photonic crystals, also superluminal group velocities and photon tunnelling have been measured [6–9].

The theory for pulse propagation in homogeneous dielectric media is extensively treated in [10–12]. Due to dispersion and absorption in the guiding medium, a pulse separates into distinct parts [11,12] in configuration space. Its wavefront propagates at the vacuum speed of light. Immediately behind it, the Sommerfeld precursor [11,12] emerges. The amplitude of this precursor is very small as compared to the applied pulse and its period is of the order of $10^{-19}$ s, both depending on material constants, propagation distance and time. Behind this precursor, the ultraviolet Brillouin precursor [11,12] emerges. Both precursors have been observed for microwaves [13] transmitted through guiding structures that have dispersion characteristics similar to those for dielectrics and for optical pulses [14,15] in water and in GaAs. Behind the Brillouin precursor, the period of the transmitted signal tunes to the applied pulse period which marks the transmission of the main part of the pulse.

Instead of the exponential amplitude decay with propagation distance for the main part of the pulse, its Sommerfeld precursor amplitude decreases roughly with the inverse square root of propagation distance [11,12]. This long range persistence may allow for applications of precursors to underwater communication or medical imaging [16]. In this paper, the Sommerfeld precursor is calculated after transmission through an $N$-layer medium, serving as a prototype of an inhomogeneous medium.

* Corresponding author. Tel.: +31 0 503634958.
*E-mail address:* r.uitham@rug.nl (R. Uitham).

0030-4018/$ - see front matter © 2006 Elsevier B.V. All rights reserved.
doi:10.1016/j.optcom.2005.12.077

This paper has been organized as follows. In Section 2 the $N$-layer medium is modelled. Section 3 is devoted to the applied pulse. A brief review of the plane wave transmission coefficient for the $N$-layer medium is given in Section 4. In Section 5, we will determine the wavefront of the transmitted pulse and in Section 6 the transmitted pulse immediately behind the wavefront, the Sommerfeld precursor, is investigated. The influence of the layered inhomogeneous medium structure onto this precursor is discussed in Section 7. We conclude in Section 8. In the appendix, the accuracy of the Sommerfeld precursor description is estimated.

## 2. Model for the $N$-layer medium

In Fig. 1 our model for the rectangular one-dimensional $N$-layer medium is depicted and in this section the spatial dependence of its refractive index is given. Each of the layers $\lambda = 1, \ldots, N$ contains two homogeneous dielectric slabs of widths $a$ and $b$ such that

$$a + b = \Lambda. \tag{1}$$

These slabs have refractive indices $n_a$ and $n_b$ respectively. The $N$-layer medium serves as a reference homogeneous medium when $n_b = n_a$ or when $b = 0$. It serves as a photonic crystal when $n_b \neq n_a$ and at the same time $b \neq 0$. It is placed in a surrounding homogeneous medium with refractive index $n_s$. The media are infinitely extended in the $yz$-plane. A medium with refractive index $n_j$ ($j = a$, $b$, $s$) is referred to as medium $j$.

Now the frequency dependence of the refractive indices of the media will be characterized. The atoms of medium $j$ have $m_j$ electronic resonances and $f_{rj}$ and $\gamma_{rj}$ denote the oscillator strength and absorption parameter corresponding to the $r$th resonance at angular frequency $\omega_{rj}$. The oscillator strengths satisfy the Thomas–Reiche–Kuhn sum rule [17, p. 261],

$$\sum_{r=1}^{m_j} f_{rj} = 1, \tag{2}$$

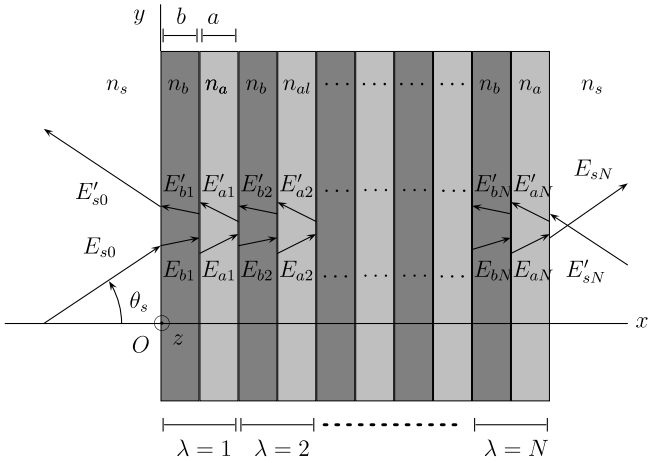


Fig. 1. Model for a one-dimensional photonic crystal with electric fields.

to be used in Section 6. The plasma angular frequency of medium $j$ is $\omega_{pj}$. For the dependence of the refractive index on the angular frequency $\omega$ of the electromagnetic field, the Lorentz model for atomic polarization and the Clausius–Mosotti relation [17, p. 266] have been used to give

$$n_j(\omega) = \left(1 + \frac{2}{3}\sum_{r=1}^{m_j} \frac{f_{rj}\omega_{pj}^2}{\omega_{rj}^2 - \omega^2 - \mathrm{i}\gamma_{rj}\omega}\right)^{1/2} \times \left(1 - \frac{1}{3}\sum_{r=1}^{m_j} \frac{f_{rj}\omega_{pj}^2}{\omega_{rj}^2 - \omega^2 - \mathrm{i}\gamma_{rj}\omega}\right)^{-1/2}. \tag{3}$$

In Fig. 2 the frequency dependence of the real and imaginary parts of a typical refractive index $n_e$ of the form of Eq. (3) is illustrated for a homogeneous example medium $e$ with 10 electron resonances ($m_e = 10$). The used values for $n_e$ are a plasma frequency $\omega_{pe} = 2.4 \times 10^{16}\mathrm{s}^{-1}$ and ten electron resonances at $\omega_{re} = r \times 10^{16}\ \mathrm{s}^{-1}$ with all oscillator strengths equal, $f_{re} = 0.1$ and absorption parameters $\gamma_{re} = (20 + r) \times 10^{14}\ \mathrm{s}^{-1}$. As well, the first order expansion of $n_e$ about infinite frequency,

$$n_e^1(\omega) = 1 - \frac{\omega_{pe}^2}{2\omega^2} \tag{4}$$

has been plotted, since this approximation will be used in the Sommerfeld precursor theory. Before proceeding to the precursor, the applied pulse is specified in the following section.

## 3. Applied pulse

The rectangular pattern in the variation of the optical properties throughout space, as imposed by the $N$-layer medium described in the previous section naturally favors the use of a cartesian coordinate system. The entrance plane defines the origin of the $x$-axis and the other two coordinates are chosen such that a right-handed coordinate system is obtained.

The electromagnetic fields propagate in the $xy$-plane into the directions of the arrows (see Fig. 1) and have transverse polarization such that $\mathbf{E}_{j\lambda}^{(\prime)} = E_{j\lambda}^{(\prime)}\hat{\mathbf{z}}$. Unprimed fields propagate forwards and primed fields propagate backwards with respect to the $x$-axis. The $N$-layer medium is irradiated from the left with a one-dimensional plane wave packet $E_{s0}$. The applied pulse is specified such that it propagates under an angle $\theta_s$ with the $x$-axis. The propagation

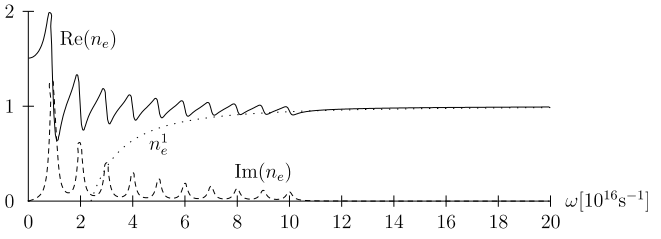


Fig. 2. Real and imaginary parts of the example refractive index. The dotted line is its first order expansion of $n_e$ about infinite frequency.

axis of the pulse in medium $s$ is therefore related to the $xy$-coordinate system as

$$\sigma_s = x\cos\theta_s + y\sin\theta_s. \tag{5}$$

The propagation angles in other media for a wave component at frequency $\omega$ can be derived from Fresnel's equation,

$$n_j(\omega)\sin\theta_j(\omega) = n_s(\omega)\sin\theta_s. \tag{6}$$

Decompose the time-dependence of the fields in the complete basis of exponentials,

$$E^{(\prime)}_{j\lambda}(t,x,y) = \int \mathrm{d}\omega \tilde{E}^{(\prime)}_{j\lambda}(\omega;x,y)\mathrm{e}^{-\mathrm{i}\omega t}, \tag{7}$$

where

$$\tilde{E}^{(\prime)}_{j\lambda}(\omega;x,y) = \frac{1}{2\pi}\int \mathrm{d}t E^{(\prime)}_{j\lambda}(t,x,y)\mathrm{e}^{\mathrm{i}\omega t}. \tag{8}$$

All time-harmonic components satisfy the wave-equation, which reads in a cartesian coordinate system as

$$\left(\frac{n_j(\omega)^2}{c^2}\frac{\partial^2}{\partial t^2} - \frac{\partial^2}{\partial x^2} - \frac{\partial^2}{\partial y^2}\right)\tilde{E}^{(\prime)}_{j\lambda}(\omega;x,y)\mathrm{e}^{-\mathrm{i}\omega t} = 0, \tag{9}$$

where $c$ is the speed of light in vacuum. For the applied field $E_{s0}$, we allow only for plane wave solutions that propagate in the above specified direction. This gives

$$E_{s0}(t,\sigma_s) = \int \mathrm{d}\omega \tilde{E}_{s0}(\omega)\mathrm{e}^{-\mathrm{i}\omega t + \mathrm{i}k^s(\omega)\sigma_s}, \tag{10}$$

where

$$\tilde{E}_{s0}(\omega) = \frac{1}{2\pi}\int \mathrm{d}t E_{s0}(t,\sigma_s = 0)\mathrm{e}^{\mathrm{i}\omega t} \tag{11}$$

is the spectral density of the applied field at the line $\sigma_s = 0$, see Fig. 3. Further,

$$k^j = \sqrt{\mathbf{k}^j\cdot\mathbf{k}^j}, \tag{12}$$

where $\mathbf{k}^j = (k^j_x, k_y, 0)$ with

$$k_y = \frac{\omega}{c}n_s(\omega)\sin\theta_s,$$

$$k^j_x = \left(\frac{\omega^2}{c^2}n_j(\omega)^2 - k_y^2\right)^{1/2} = \frac{\omega}{c}\sqrt{n_j(\omega)^2 - n_s(\omega)^2\sin^2\theta_s}. \tag{13}$$

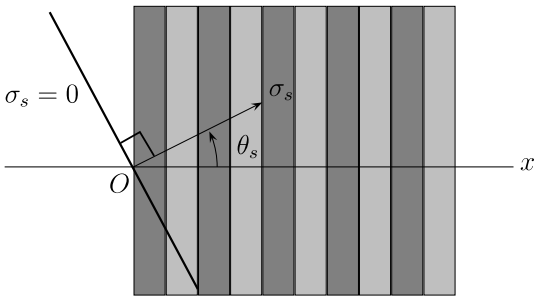


Fig. 3. The line $\sigma_s = 0$ is the wavefront at $t = 0$ and the applied field propagates along the $\sigma_s$-axis.

Now the spectral density of Eq. (11) will be calculated for a generic pulse of finite time duration. The applied field is constructed such that at $\sigma_s = 0$, it is zero at times $t \notin [0,T]$ with $T > 0$ finite,

$$E_{s0}(t,\sigma_s = 0) = \mathscr{E}_{s0}(t)I_{[0,T]}(t). \tag{14}$$

Here $\mathscr{E}_{s0}(0) = \mathscr{E}_{s0}(T) = 0$ and

$$I_{[0,T]}(t) = \begin{cases} 1 & \text{for} \quad t \in [0,T], \\ 0 & \text{for} \quad t \notin [0,T]. \end{cases} \tag{15}$$

A convenient basis for $\mathscr{E}_{s0}(t)$ is a trigonometric one,

$$\mathscr{E}_{s0}(t) = \sum_{m=0}^{\infty}\tilde{\mathscr{E}}_{s0}(\omega_m)\sin\omega_m t$$

$$\tilde{\mathscr{E}}_{s0}(\omega_m) = \frac{2}{T}\int_0^T \mathrm{d}t\mathscr{E}_{s0}(t)\sin\omega_m t. \tag{16}$$

Here

$$\omega_m = \frac{m\pi}{T} \tag{17}$$

in order for $\mathscr{E}_{s0}(t)$ to vanish at $t = 0,T$. The coefficients $\tilde{\mathscr{E}}_{s0}(\omega_m)$ are the spectral weights of the unmodulated infinitely long lasting $T$-periodic signal $\mathscr{E}_{s0}(t)$ at its carrier angular frequencies $\omega_m$. Only pulses with finite carrier frequencies are considered,

$$\tilde{\mathscr{E}}_{s0}(\omega_m) = 0 \quad \text{for} \quad m > M, \tag{18}$$

where $M$ is a nonnegative integer. With Eq. (16), the spectral density Eq. (11) of the applied field at $\sigma_s = 0$ becomes

$$\tilde{E}_{s0}(\omega) = \frac{1}{2\pi}\sum_m \frac{\omega_m\tilde{\mathscr{E}}_{s0}(\omega_m)}{\omega^2 - \omega_m^2}\left((-1)^m\mathrm{e}^{\mathrm{i}\omega T} - 1\right). \tag{19}$$

Eq. (10) with (19) together describe a generic plane wave pulse of finite time duration that propagates under an angle $\theta_s$ with the $x$-axis in the surrounding medium. For an applied plane wave packet $E_{s0}$, the transmitted field $E_{sN}$ is obtained from it via the plane wave transmission coefficient for the $N$-layer medium, which is calculated in the next section.

## 4. $N$-layer medium plane-wave transmission coefficient

For plane wave transverse polarized fields, the temporal Fourier coefficients of the electric fields in homogeneous media $a$ surrounding a vertical homogeneous slab $b$, the fields being evaluated at a mutual horizontal distance $\Lambda$, are related via the corresponding unimodular transfer matrix $M$ [18,19],

$$\begin{pmatrix}\tilde{E}_{a\lambda}\\ \tilde{E}'_{a\lambda}\end{pmatrix} = M\begin{pmatrix}\tilde{E}_{a\lambda-1}\\ \tilde{E}'_{a\lambda-1}\end{pmatrix} = \begin{pmatrix}A & D\\ B & C\end{pmatrix}\begin{pmatrix}\tilde{E}_{a\lambda-1}\\ \tilde{E}'_{a\lambda-1}\end{pmatrix}. \tag{20}$$

The transfer matrix is constructed from propagation and dynamical matrices,

$$P_j = \begin{pmatrix}\mathrm{e}^{\mathrm{i}k^j_x j} & 0\\ 0 & \mathrm{e}^{-\mathrm{i}k^j_x j}\end{pmatrix}, \quad \Delta_j = \begin{pmatrix}1 & 1\\ ck^j_x/\omega & -ck^j_x/\omega\end{pmatrix}, \tag{21}$$

as $M = P_a\Delta_a^{-1}\Delta_b P_b \Delta_b^{-1}\Delta_a$. The latter in Eq. (21) is given here for transverse electric polarization. This gives the entries of $M$ as

$$\begin{aligned} A &= \mathrm{e}^{\mathrm{i}k_x^a a}\left(\cos k_x^b b + \frac{\mathrm{i}}{2}\left(\frac{k_x^b}{k_x^a}+\frac{k_x^a}{k_x^b}\right)\sin k_x^b b\right),\\ B &= \frac{\mathrm{i}}{2}\mathrm{e}^{\mathrm{i}k_x^a \alpha}\left(\frac{k_x^b}{k_x^a}-\frac{k_x^a}{k_x^b}\right)\sin k_x^b b,\\ C &= \frac{-\mathrm{i}}{2}\mathrm{e}^{-\mathrm{i}k_x^a a}\left(\frac{k_x^b}{k_x^a}-\frac{k_x^a}{k_x^b}\right)\sin k_x^b b,\\ D &= \mathrm{e}^{-\mathrm{i}k_x^a a}\left(\cos k_x^b b - \frac{\mathrm{i}}{2}\left(\frac{k_x^b}{k_x^a}+\frac{k_x^a}{k_x^b}\right)\sin k_x^b b\right). \end{aligned} \tag{22}$$

The fields at both sides from the $N$-layer medium in a surrounding homogeneous medium $a$ are related via

$$\begin{pmatrix}\tilde{E}_{aN}\\ \tilde{E}'_{aN}\end{pmatrix} = \begin{pmatrix}A_N & B_N\\ C_N & D_N\end{pmatrix}\begin{pmatrix}\tilde{E}_{a0}\\ \tilde{E}'_{a0}\end{pmatrix},\quad \begin{pmatrix}A_N & B_N\\ C_N & D_N\end{pmatrix} \equiv \begin{pmatrix}A & B\\ C & D\end{pmatrix}^N. \tag{23}$$

The entries $A_N,\ldots,D_N$ can be found by solving Eq. (20) with the discrete Mellin transform method [18]. One finds

$$\begin{aligned} A_N &= A\frac{\alpha^N-\alpha^{-N}}{\alpha-\alpha^{-1}} - \frac{\alpha^{N-1}-\alpha^{-N+1}}{\alpha-\alpha^{-1}},\\ B_N &= B\frac{\alpha^N-\alpha^{-N}}{\alpha-\alpha^{-1}},\quad C_N = C\frac{\alpha^N-\alpha^{-N}}{\alpha-\alpha^{-1}},\\ D_N &= D\frac{\alpha^N-\alpha^{-N}}{\alpha-\alpha^{-1}} - \frac{\alpha^{N-1}-\alpha^{-N+1}}{\alpha-\alpha^{-1}}. \end{aligned} \tag{24}$$

Here $\alpha^{\pm 1} = \frac{1}{2}(A+D) \pm \frac{1}{2}\sqrt{(A+D)^2-4}$ are the eigenvalues of the transfer matrix. The correction of the surrounding medium $a$ to a medium $s$ gives

$$\begin{pmatrix}\tilde{E}_{sN}\\ \tilde{E}'_{sN}\end{pmatrix} = \Delta_s^{-1}\Delta_a\begin{pmatrix}A_N & B_N\\ C_N & D_N\end{pmatrix}\Delta_a^{-1}\Delta_s\begin{pmatrix}\tilde{E}_{s0}\\ \tilde{E}'_{s0}\end{pmatrix} \tag{25}$$

and the transmission coefficient of the $N$-layer medium follows as ($f \equiv \frac{k_x^a}{k_x^s}$)

$$\begin{aligned} t_N &\equiv \left(\frac{\tilde{E}_{sN}}{\tilde{E}_{s0}}\right)\Bigg|_{\tilde{E}'_{sN}=0}\\ &= \frac{-4f}{(f-1)^2 A_N - (f^2-1)(C_N-B_N) - (f+1)^2 D_N}. \end{aligned} \tag{26}$$

Via the transmission of the applied pulse of Section (3) through the $N$-layer medium, we arrive at the transmitted pulse $E_{sN}$. In the following section, we determine the wavefront and in the section thereafter, we investigate its shape immediately behind the wave front.

## 5. Wavefront of the transmitted signal

In order to describe the behavior of the transmitted pulse immediately behind the wavefront, we will first determine the wavefront itself. Hereto reconsider the expression for the applied pulse, Eq. (10). Its integrand is analytic at the real axis and in the upper half frequency plane. Hence the integration path may freely be deformed from the real axis into path $S$, see Fig. 4. This path follows the real axis up to a semicircle detour in the upper half plane with center $\omega = 0$ and radius $\Omega$. With $S$ as integration path, traversed from $\omega = -\infty$ to $+\infty$, the transmitted pulse follows from Eqs. (10) and (26) as

$$E_{sN}(t,\sigma_s) = \int_S \mathrm{d}\omega t_N(\omega)\mathrm{e}^{-\mathrm{i}k_x^s(\omega)N\Lambda}\tilde{E}_{s0}(\omega)\mathrm{e}^{-\mathrm{i}\omega t + \mathrm{i}k^s(\omega)\sigma_s}, \tag{27}$$

where the factor $\mathrm{e}^{-\mathrm{i}k_x^s(\omega)N\Lambda}$ matches the phase of the field at $x = N\Lambda$.

From Eq. (3) it follows that $n_j(|\omega| = \infty) = 1$. Hence spectral components at infinite frequencies experience the $N$-layer medium as if it were a vacuum. So, of all frequency components, these are the fastest propagating components. When present in the pulse, solely these infinite frequency components will form the wavefront at positions ahead of the starting line $\sigma_s = 0$, i.e. after propagation.

The contribution from these fast propagating frequency components to the complete field, Eq. (27), can be isolated by choosing the integration path radius $\Omega$ very large with respect to the frequency parameters of the refractive indices,

$$\Omega^{-1}\max(\omega_{pj},\omega_j,\gamma_j) = \epsilon, \tag{28}$$

where $\epsilon$ is a small positive real number: $0 < \epsilon \ll 1$. The radius $\Omega$ is kept finite in order for the integral in Eq. (27) to be well-defined for all values of $(t,\sigma_s)$. When using this large radius $\Omega$, the refractive indices, when evaluated on $S$, are approximated accurately by their zeroth order expansions about infinite frequency, since

$$n_j(\omega)|_{\omega\in S} = 1 + \mathcal{O}(\epsilon^2). \tag{29}$$

On $S$, the transmission coefficient for the $N$-layer system is within this zeroth order approximation equal to

$$t_N(\omega)|_{\omega\in S} \simeq t_N(\omega)|_{n_j=1} = \mathrm{e}^{\mathrm{i}\frac{\omega}{c}N\Lambda\cos\theta_s}. \tag{30}$$

Denote the fastest travelling part (or very high frequency part) of the transmitted field $E_{sN}$ of Eq. (27) as $E_{sN}^0$. The expansion of $n_j$ about infinite frequency corresponds to

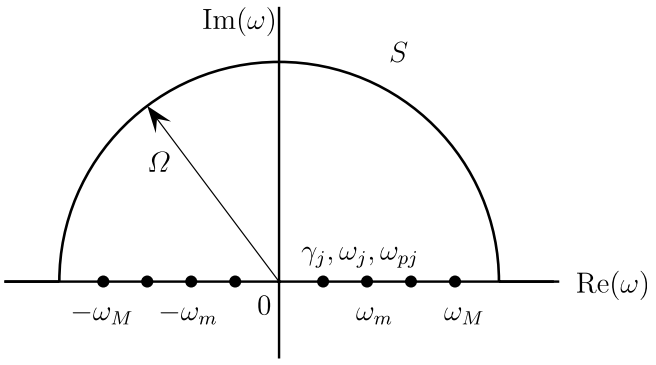


Fig. 4. The path $S$ together with all frequency parameters in the complex frequency plane.

an expansion of the transmitted field about $E^0_{sN}$, which equals

$$E^0_{sN}(t,\sigma_s) = \int_S \mathrm{d}\omega t_N(\omega)\mathrm{e}^{-\mathrm{i}k^s_x(\omega)N\Lambda}\tilde{E}_{s0}(\omega)\mathrm{e}^{-\mathrm{i}\omega t+\mathrm{i}k^s(\omega)\sigma_s}\big|_{n_j=1} = \int_S \mathrm{d}\omega\tilde{E}_{s0}(\omega)\mathrm{e}^{-\mathrm{i}\omega\tau(t,\sigma_s)}, \tag{31}$$

where the real function

$$\tau(t,\sigma_s) \equiv t - \sigma_s/c. \tag{32}$$

When we explicate the spectral density in Eq. (31),

$$E^0_{sN}(t,\sigma_s) = \int_S \mathrm{d}\omega \sum_m \frac{\omega_m\tilde{\mathscr{E}}_{s0}(\omega_m)}{\omega^2-\omega_m^2} \times \left((-1)^m\mathrm{e}^{-\mathrm{i}\omega(\tau(t,\sigma_s)-T)} - \mathrm{e}^{-\mathrm{i}\omega\tau(t,\sigma_s)}\right), \tag{33}$$

it is clear that both exponents have arbitrary large negative real parts (for an arbitrary large radius $\Omega$) when $\tau<0$. The contribution from the part of the integration near and at the real axis is arbitrary small as well since the spectral density $\tilde{E}_{s0}(\omega)$ behaves as $\frac{1}{\omega^2}$ for $|\omega|$ large. When $0<\tau<T$, the integration path for the first term in Eq. (33) can still be taken as $S$ in order to have exponential decay with $\Omega$. For the second term in Eq. (33), the path should be deformed into a very large semicircle in the lower half frequency plane, but then one encounters the branch lines from the refractive index and the poles at $\omega=\pm\omega_m$ (although the complete expression Eq. (33) has no poles at these positions, the separate terms do), giving a nonzero signal for $\tau>0$. Hence the wavefront is given by the equation $\tau=0$. The quantity $\tau$ is therefore the time elapse after the wave-front has passed. Now that the location of the wavefront has been determined, we can proceed to the transmitted pulse immediately behind the wavefront.

## 6. Sommerfeld precursor

The Sommerfeld precursor starts immediately behind the wavefront. Since the wavefront serves as a reference line, it is convenient to use the set of independent coordinates $(\tau,\sigma_s)$ instead of the set $(t,\sigma_s)$. In terms of these, the complete transmitted field, Eq. (27), reads as

$$E_{sN}(\tau,\sigma_s) = \int_S \mathrm{d}\omega t_N\mathrm{e}^{-\mathrm{i}\frac{\omega}{c}k^s_xN\Lambda}\mathrm{e}^{\mathrm{i}(k^s-\frac{\omega}{c})\sigma_s}\mathrm{e}^{-\mathrm{i}\omega\tau}\tilde{E}_{s0}. \tag{34}$$

Here $S$ is still the integration path with a semicircle in the upper half plane, see Fig. 4. The zeroth order expansions about infinite frequency, were used to determine the wavefront. In order to derive the Sommerfeld precursor, their first order expansions will be used,

$$n_j(\omega) = 1 - \frac{\omega^2_{pj}}{2\omega^2}. \tag{35}$$

The refractive indices are contained in the expression for the transmitted wave, Eq. (34), through the factors

$$t_N\mathrm{e}^{-\mathrm{i}k^s_xN\Lambda}\ \text{(a)} \quad \text{and} \quad \mathrm{e}^{\mathrm{i}(k^s_x-\frac{\omega}{c})\sigma_s}\ \text{(b)} \tag{36}$$

and the high frequency behavior of these factors will be determined in the following.

With Eq. (35), the high frequency behavior of Eq. (36b) immediately follows as

$$\mathrm{e}^{\mathrm{i}(k^s_x-\frac{\omega}{c})\sigma_s}\big|_{n_s(\omega)=1-\frac{\omega^2_{ps}}{2\omega^2}} = \mathrm{e}^{-\mathrm{i}\frac{\omega^2_{ps}\sigma_s}{2c}\frac{1}{\omega}}. \tag{37}$$

For the manipulation of Eq. (36a), it is convenient to consider another expanded form for $t_N$. Let $r_{jj'}$ denote the single boundary reflection factor for an electric field that propagates in medium $j$ and is reflected at a boundary with medium $j'$ and let $t_{jj'}$ denote the corresponding single boundary transmission factor. For transverse electric polarization,

$$r_{jj'} = \frac{k^j_x - k^{j'}_x}{k^j_x + k^{j'}_x}, \quad t_{jj'} = 1 + r_{jj'}, \tag{38}$$

see [20]. The $x$-component of the propagation factor over a distance $j$ through medium $j$ is

$$p_j = \mathrm{e}^{\mathrm{i}k^j_xj}. \tag{39}$$

The slab $a$-transfer matrix elements of Eq. (22) can be expressed in these factors,

$$\begin{aligned} A &= t_{ab}t_{ba}p_a(p_b - r^2_{ab}p_b^{-1}),\\ B &= r_{ba}t^{-1}_{ab}t^{-1}_{ba}p_a(p_b - p_b^{-1}),\\ C &= r_{ab}t^{-1}_{ab}t^{-1}_{ba}p_a^{-1}(p_b - p_b^{-1}),\\ D &= t^{-1}_{ab}t^{-1}_{ba}p_a^{-1}(p_b^{-1} - r^2_{ab}p_b) \end{aligned} \tag{40}$$

and we can choose to expand the transmission coefficient $t_N$ in powers of $p$, which is a propagation path-length ordering of the wave within the $N$-layer medium. The first few terms of this path-length expansion of $t_N$ are

$$t_N(p,r,t) = t_{sb}t_{ab}^{N-1}(t_{ba}p_ap_b)^Nt_{as}(1 + r_{ba}r_{bs}p_b^2 + (N-1)r^2_{ab}p_a^2 + (N-1)r^2_{ba}p_b^2 + (N-1)r^2_{ab}p_a^2 + r_{as}r_{ab}p_a^2 + \cdots). \tag{41}$$

The paths corresponding to these terms are sketched in Fig. 5. The transmitted signal immediately behind the wavefront at $\tau=0$ clearly consists from the waves that have followed the path without internal reflections in Fig. (5). Furthermore the contributions from other paths (with internal reflections) can be neglected for the high-frequency components as will be shown now. With Eq. (35), the high-frequency approximation of the reflection coefficient, Eq. (38), follows as

$$r_{jj'}(\omega)|_{\omega\in S} = \frac{\omega^2_{pj'} - \omega^2_{pj}}{4\cos^2\theta_s}\frac{1}{\omega^2} + \mathscr{O}(\epsilon^4) \tag{42}$$

with $\epsilon$ from Eq. (28). Here (and in the following) the sum rule, Eq. (2), has been used. From Eqs. (41) and (42) it follows that transmitted waves that have experienced reflections within the $N$-layer medium give contributions to $t_N$ that are at least quadratic in the reflection coefficients. Therefore, on the integration path $S$, they give contributions of order $\epsilon^4$, so

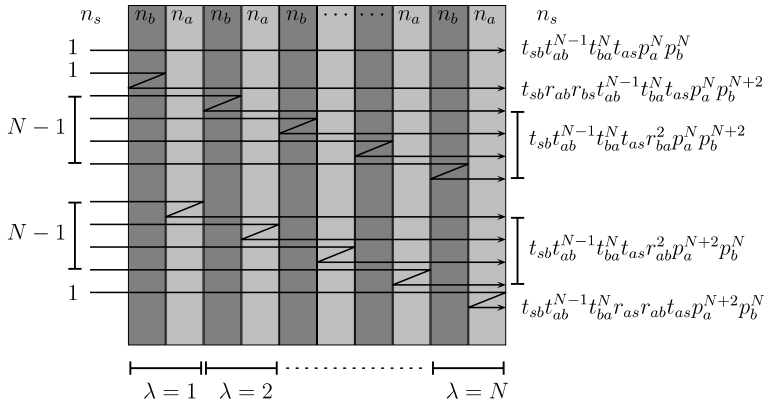


Fig. 5. First few terms in the path-length ordered form of the transmission coefficient.

$$t_N(\omega)|_{\omega\in S} = t_{sb}t_{ab}^{N-1}t_{ba}^{N}t_{as}p_a^N p_b^N + \mathcal{O}(\epsilon^4). \tag{43}$$

The $\mathcal{O}(\epsilon^4)$ terms are very small with respect to the wave that has not experienced internal reflections and may be omitted when attention is restricted to positions immediately behind the wavefront. The dominant term of Eq. (36a) at large frequencies is thus

$$t_{sb}t_{ab}^{N-1}t_{ba}^{N}t_{as}p_a^N p_b^N \mathrm{e}^{-\mathrm{i}k_x^s N\Lambda}\big|_{\omega\in S} \simeq \mathrm{e}^{\frac{\mathrm{i}Na\left(\omega_{ps}^2-\omega_{pa}^2\right)+\mathrm{i}Nb\left(\omega_{ps}^2-\omega_{pb}^2\right)}{2c\cos\theta_s}\frac{1}{\omega}}. \tag{44}$$

At very large frequencies such that $|\omega| \gg \omega_M$, the spectral density, Eq. (19), may be expanded to first order as well,

$$\tilde{E}_{s0}(\omega) = -\frac{1}{2\pi}\sum_m \frac{\omega_m \tilde{\mathscr{E}}_{s0}(\omega_m)}{\omega^2} \tag{45}$$

and the dominant contribution to the initially transmitted field, Eq. (34) follows as the Sommerfeld precursor

$$S_{sN}(\tau,\sigma_s) = -\frac{1}{2\pi}\sum_m \omega_m \tilde{\mathscr{E}}_{s0}(\omega_m)\int_S \mathrm{d}\omega \frac{\mathrm{e}^{-\mathrm{i}\omega\tau-\mathrm{i}\xi(\sigma_s)/\omega}}{\omega^2}, \tag{46}$$

where the real function

$$\xi(\sigma_s) = N\frac{a\omega_{pa}^2 + b\omega_{pb}^2 - \Lambda\omega_{ps}^2}{2c\cos\theta_s} + \frac{\omega_{ps}^2}{2c}\sigma_s. \tag{47}$$

For $\tau > 0$, the absolute value of the integrand in Eq. (46) grows exponentially with the radius $\Omega$ of the semicircle part of $S$. This does not necessarily imply that the integral diverges, since also the oscillation frequency of the integrand along the semicircle increases. We will next show that the integral actually converges in the limit $\Omega \to \infty$. The steps taken in the following are merely a repetition of the work in [11] in order to perform the integration.

Consider the path $\bar{S}$, which is obtained from path $S$ by reflection about the point $\omega = 0$. On $\bar{S}$, Eq. (46) is arbitrary small (for arbitrary large $\Omega$) for $\tau > 0$, so this path $\bar{S}$ may be added to $S$ in Eq. (46). The integration over $\bar{S}$ is chosen to run from $\omega = +\infty$ to $\omega = -\infty$. When $\bar{S}$ is added to $S$, one obtains a circular path, denoted as $C$, which is traversed clockwise. With reversion to counterclockwise traversing of $C$, and with rewriting the exponent of Eq. (46), one obtains

$$S_{sN}(\tau,\sigma_s) = \frac{1}{2\pi}\sum_m \omega_m \tilde{\mathscr{E}}_{s0}(\omega_m)\oint_C \mathrm{d}\omega \frac{\mathrm{e}^{-\mathrm{i}\sqrt{\xi(\sigma_s)\tau}\left(\omega\sqrt{\frac{\tau}{\xi(\sigma_s)}}+\frac{1}{\omega}\sqrt{\frac{\xi(\sigma_s)}{\tau}}\right)}}{\omega^2}. \tag{48}$$

Change the integration variable from $\omega$ to $\phi = -\mathrm{i}\sqrt{\frac{\tau}{\xi}}\omega$ to identify the initially transmitted electric field as

$$S_{sN}(\tau,\sigma_s) = \sum_m \omega_m \tilde{\mathscr{E}}_{s0}(\omega_m)\sqrt{\frac{\tau}{\xi(\sigma_s)}}J_1\left(2\sqrt{\xi(\sigma_s)\tau}\right). \tag{49}$$

Here $J_1$ is the Bessel function of the first kind and order. Eq. (49) has exactly the same form as the expression for the Sommerfeld precursor after transmission through a homogeneous medium [11]. In the next section we will discuss the changes due to the layered structure of the medium.

## 7. Discussion

First the transmission of a pulse through a homogeneous medium and transmission through an $N$-layer medium will be compared. For transmission over a horizontal distance $N\Lambda$ through a homogeneous medium $a$ and for initial propagation along the $\sigma_s$-axis in a vacuum surrounding medium $s$, the function $\xi$ in the expression for the initially transmitted field, Eq. (49), simplifies to

$$\xi_{\mathrm{ref}} \equiv \xi|_{n_b=n_a,n_s=1} = \frac{N\Lambda\omega_{pa}^2}{2c\cos\theta_s}. \tag{50}$$

Note that the function $\xi$ of Eq. (47) is symmetric in the media $a$ and $b$. So medium $b$ could have played the rôle of reference medium as well. For the $N$-layer system in between vacuum, the function $\xi$ is

$$\xi = N\frac{a\omega_{pa}^2 + b\omega_{pb}^2}{2c\cos\theta_s}. \tag{51}$$

So the plasma frequency squared for a homogeneous medium is simply replaced by the spatial average of the plasma frequency squared of the $N$-layer medium.

The influence of the perturbing medium $b$ on the Sommerfeld precursor will be explicated somewhat further. The relative slabwidth of slab $b$ is

$$\beta = \frac{b}{\Lambda} \tag{52}$$

and the relative difference of the squared plasma frequencies is

$$\Delta = \frac{\omega_{pb}^2 - \omega_{pa}^2}{\omega_{pa}^2}. \tag{53}$$

In terms of these parameters, Eq. (51) reads as

$$\xi = (1+\delta)\xi_{\mathrm{ref}}; \quad \delta = \beta\Delta \tag{54}$$

and the Sommerfeld precursor field, Eq. (49), reads as

$$S_{sN}(\tau) = \sum_m \omega_m \tilde{\mathscr{E}}_{s0}(\omega_m) \times \sqrt{\frac{\tau}{(1+\delta)\xi_{\mathrm{ref}}}} J_1\left(2\sqrt{(1+\delta)\xi_{\mathrm{ref}}\tau}\right). \tag{55}$$

Fig. 6 shows the field transmitted field of Eq. (55) for perpendicular incidence ($\theta_s = 0$) and transmission through several $N$-layer media with $N = 100$ $\Lambda = 600$ nm. The reference medium $a$ is made of silicon which has $\omega_{pa} = 2.4 \times 10^{16}$ $\mathrm{s}^{-1}$ [21, p. 278]. The effect on the precursor field of changing a homogeneous medium into a photonic structure is captured in the parameter $\delta$. There are three distinguishable situations:

- $\delta = 0$ This corresponds to either zero relative slabwidth $\beta = 0$ or equal plasma frequencies, $\omega_{pb} = \omega_{pa} = 2.4 \times 10^{16}$ $\mathrm{s}^{-1}$. This trivial situation represents the homogeneous reference medium $a$ and the corresponding initially transmitted field is given by the solid line.
- $\delta > 0$ This is obtained when $\omega_{pb} > \omega_{pa}$ together with nonzero $\beta$. The amplitude and period of the initially transmitted field have decreased with respect to the transmitted field through the reference medium. This situation holds for the dotted line ($\omega_{pb} = 3.0 \times 10^{16}$ $\mathrm{s}^{-1} > \omega_{pa}, \beta = \frac{1}{2}$).
- $\delta < 0$ When on the other hand $\omega_{pb} < \omega_{pa}$ and $\beta \neq 0$ then the amplitude and period increase with respect to the reference medium case, as shown by the dashed line ($\omega_{pb} = 1.8 \times 10^{16}$ $\mathrm{s}^{-1} < \omega_{pa}, \beta = \frac{1}{2}$).

The effects increase with increasing $\beta$. The extreme case $\delta = -1$ is obtained from putting $\beta = 1$ and $\omega_{pb} = 0$. The $N$-layer medium has reduced to a complete vacuum and gives for the transmitted field

$$\lim_{\delta\to-1} \sum_m \omega_m \tilde{\mathscr{E}}_{s0}(\omega_m) \sqrt{\frac{\tau}{\xi_a(1+\delta)}} J_1\left(2\sqrt{\xi_a(1+\delta)\tau}\right) = \sum_m \tilde{\mathscr{E}}_{s0}(\omega_m)\omega_m\tau. \tag{56}$$

This is indeed the approximation for the applied field, Eq. (16), propagated through vacuum valid for $\omega_M\tau \ll 1$.

At last, the initial amplitude of the transmitted Sommerfeld precursor, Eq. (49), is compared to the applied signal amplitude, Eq. (16). This is done for transmission through the homogeneous reference medium $a$ over a distance $N\Lambda = 6.00 \times 10^{-5}$ m. For perpendicular incidence onto a silicon dielectric, Eq. (50) gives $\xi_{\mathrm{ref}} = 5.76 \times 10^{19}$ $\mathrm{s}^{-1}$. The first maximum of $J_1$ is at $2\sqrt{\xi\tau} = 1.84$ and has the value 0.582. At this maximum, $\tau = 1.47 \times 10^{-20}$ s. For simplicity take an applied pulse with only one single optical carrier angular frequency $\omega_M = 3.00 \times 10^{15}$ $\mathrm{s}^{-1}$ and amplitude $\tilde{\mathscr{E}}_{s0}(\omega_M)$,

$$E_{s0}(t, \sigma_s = 0) = I_{[0,T]}(t)\tilde{\mathscr{E}}_{s0}(\omega_M)\sin\omega_M t. \tag{57}$$

For perpendicular incidence, $\sigma_s = 0$ coincides with the entrance line of the medium, $x = 0$. Hence at the first maximum, Eq. (49) gives $S_{sN} = 2.79 \cdot 10^{-5}\tilde{\mathscr{E}}_{s0}(\omega_M)$. Therefore the initial amplitude of the Sommerfeld precursor for this specific applied field transmitted through the reference medium is very small compared to the amplitude of the corresponding applied pulse.

## 8. Conclusion

The wavefront of a pulse that propagates in a dielectric medium is constructed from the infinite frequency components of that pulse, since the electrons of the medium are inert and no polarization can be induced. When a homogeneous dielectric medium is replaced by a rectangular photonic crystal that consists of layers of the same type of media, the wavefront therefore still propagates at the vacuum speed of light.

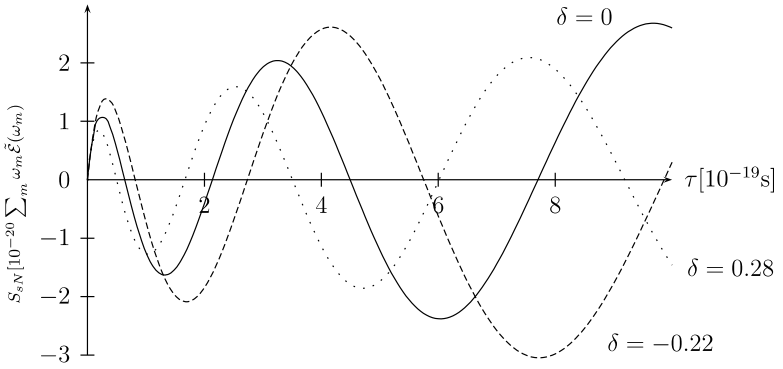


Fig. 6. Transmitted field through a homogeneous Si medium (solid line) and through two photonic crystals of the same length, but with different plasma frequencies.

The Sommerfeld precursor results from very high frequency components of the pulse, which experience the medium as if it were almost vacuum. This precursor immediately follows the wavefront of the transmitted pulse. Although the individual frequency components of the applied pulse experience a frequency-dependent refraction at each interface within the photonic crystal, after transmission a Sommerfeld precursor emerges of the same shape as for the homogeneous medium. The only difference is that in the expression for the Sommerfeld precursor, the plasma frequency squared for the case of a homogeneous medium is replaced by the spatial average of the plasma frequency squared of the layered medium.

**Acknowledgements**

The authors would like to thank Professor J. Knoester for his useful suggestions. This research is supported by NanoNed, a national nanotechnology programme coordinated by the Dutch Ministry of Economic Affairs.

**Appendix A**

In this appendix the accuracy of the Sommerfeld precursor approximation to the field is estimated in the time domain. For brevity a plane wave of one single carrier frequency $\omega_c$ is considered which is perpendicularly incident from vacuum at $x<0$ onto a half-infinite homogeneous medium $a$ at $x>0$. This pulse has the time dependence $E(t)$ and time duration $T$ at $x=0$. The total electric field in the homogeneous medium can be written as

$$E(\tau,x)=\int_S \mathrm{d}\omega \tilde{L}(\omega;x)\tilde{S}(\omega)\mathrm{e}^{-\xi_1(x)/\omega}\mathrm{e}^{-\mathrm{i}\omega\tau}, \tag{A.1}$$

$$\tilde{L}(\omega;x)=\sum_{q=0}^{\infty}\frac{\omega_c^{2q}}{\omega^{2q}}\exp\left(-\mathrm{i}\sum_{r=2}^{\infty}\frac{\xi_r(x)}{\omega^r}\right),\quad \tilde{S}(\omega)=\frac{1}{2\pi}\frac{\omega_c\tilde{E}(\omega_c)}{\omega^2},$$

where $\tau=t-x/c$, $\tilde{E}(\omega_c)=\frac{2}{T}\int_0^T \mathrm{d}t E(t)\sin\omega_c t$ and

$$\xi_r(x)\equiv -\frac{x}{c}\frac{1}{(r+1)!}\left.\frac{\mathrm{d}^{r+1}\eta(v)}{\mathrm{d}v^{r+1}}\right|_{v=\omega^{-1}=0}. \tag{A.2}$$

Here $\eta(v)=n(\omega)|_{\omega=v^{-1}}$ and $n(\omega)$ is the refractive index, Eq. (3), for $j=a$. Use

$$\frac{(-\mathrm{i})^{n+1}}{n!}\int_0^\tau \mathrm{d}\tau'(\tau-\tau')^n S(\tau',x) = \int_S \mathrm{d}\omega\frac{1}{\omega^{n+1}}\tilde{S}(\omega)\mathrm{e}^{-\mathrm{i}\omega\tau-\mathrm{i}\frac{\xi_1(x)}{\omega}}, \tag{A.3}$$

$$S(\tau,x)+\left(\mathrm{e}^{\frac{(-\mathrm{i})^{n+1}}{n!}\int_0^\tau \mathrm{d}\tau'(\tau-\tau')^n}-1\right)S(\tau',x) = \int_S \mathrm{d}\omega \mathrm{e}^{1/\omega^{n+1}}\tilde{S}(\omega)\mathrm{e}^{-\mathrm{i}\omega\tau-\mathrm{i}\frac{\xi_1(x)}{\omega}}, \tag{A.4}$$

to rewrite Eq. (A.1) as $E(\tau,x)=S(\tau,x)+(L*S)(\tau,x)$ where convolution is with respect to the variable $\tau$ and $L=\epsilon_1+\epsilon_2+\epsilon_1*\epsilon_2$ with

$$\epsilon_1*S(\tau,x)=\sum_{q=1}^{\infty}\omega_c^{2q}\frac{(-\mathrm{i})^{2q}}{(2q-1)!}\int_0^\tau \mathrm{d}\tau'(\tau-\tau')^{2q-1}S(\tau',x), \tag{A.5}$$

$$\epsilon_2(x)*S(\tau,x)=\left(\exp\left(-\mathrm{i}\sum_{r=2}^{\infty}\frac{\xi_r(x)(-\mathrm{i})^r}{(r-1)!}\times\int_0^\tau \mathrm{d}\tau'(\tau-\tau')^{r-1}\right)-1\right)S(\tau',x). \tag{A.6}$$

The difference between the actual electric field and the Sommerfeld approximation is the remainder $R=E-S=L*S$. We demand that for some small $\epsilon\in\mathbb{R}$,

$$\|R\|_2=\|L*S\|_2<\epsilon\|S\|_2, \tag{A.7}$$

where $\|R\|_2$ is the $L^2$-norm of the function $R$ on the interval $(0,\tau)$,

$$\|R\|_2=\sqrt{\frac{1}{\tau}\int_0^\tau \mathrm{d}\tau'|R(\tau',x)|^2}. \tag{A.8}$$

Since $L$ is linear, its norm is (see [22]) $\|L\|=\sup_{\|f\|=1}\|Lf\|$. Therefore $\|Lf\|\leqslant\|L\|$ and we may require $\|L\|_2<\epsilon$. This requirement is relaxed a little by demanding

$$\|\epsilon_1\|_2<\epsilon/2\quad\text{and}\quad\|\epsilon_2\|_2<\epsilon/2 \tag{A.9}$$

and neglecting the $\epsilon_1*\epsilon_2$-term. A typical term in $L$ is of the form

$$\begin{aligned}\left\|\frac{(-\mathrm{i})^{n+1}}{n!}\int_0^\tau \mathrm{d}\tau'(\tau'-\tau)^n\right\|_2^2 &= \left\|\left(-\mathrm{i}\int_0^\tau \mathrm{d}\tau_1\right)\left(-\mathrm{i}\int_0^{\tau_1}\mathrm{d}\tau_2\right)\cdots\left(-\mathrm{i}\int_0^{\tau_n}\mathrm{d}\tau_{n+1}\right)\right\|_2^2\\ &\leqslant\left\|\left(-\mathrm{i}\int_0^\tau \mathrm{d}\tau'\right)^{n+1}\right\|_2^2\\ &=\sup_{\|f\|=1}\frac{1}{\tau}\int_0^\tau \mathrm{d}\tau'\left(\int_0^{\tau'}\mathrm{d}\tau'' f(\tau'')\right)^{2n+2}.\end{aligned} \tag{A.10}$$

The supremum in the right-hand-side of Eq. (A.10) is found by demanding the functional

$$I[f](\tau)=\frac{1}{\tau}\int_0^\tau \mathrm{d}\tau'\left(\int_0^{\tau'}\mathrm{d}\tau'' f(\tau'')\right)^{2n+2}+\lambda(\tau)\left(\frac{1}{\tau}\int_0^\tau \mathrm{d}\tau' f(\tau')^2-1\right) \tag{A.11}$$

to be stationary under variations in $f$. Here $\lambda$ is a Lagrange multiplier. This gives $f=\pm1$ and

$$\left\|\frac{(-\mathrm{i})^{n+1}}{n!}\int_0^\tau \mathrm{d}\tau'(\tau'-\tau)^n\right\|_2\leqslant\frac{\tau^{n+1}}{\sqrt{2n+3}}. \tag{A.12}$$

Therefore

$$\|\epsilon_1\|_2 \leqslant \sum_{q=1}^{\infty} \frac{\omega_c^{2q}\tau^{2q}}{\sqrt{4q+1}} \quad \text{and}$$

$$\|\epsilon_2\|_2 \leqslant \exp\left(\sum_{r=2}^{\infty} \frac{|\xi_r(x)|\tau^r}{\sqrt{2r+1}}\right) - 1. \tag{A.13}$$

This gives

$$\sum_{q=1}^{\infty} \frac{\omega_c^{2q}\tau^{2q}}{\sqrt{4q+1}} < \epsilon/2, \quad \sum_{r=2}^{\infty} \frac{|\xi_r(x)|\tau^r}{\sqrt{2r+1}} < \epsilon/2. \tag{A.14}$$

so if

$$\omega_c\tau < \epsilon/2 \quad \text{and} \quad |\xi_2|\tau^2 = \frac{\gamma\omega_{pa}^2 x}{2c}\tau^2 < \epsilon/2, \tag{A.15}$$

then requirement Eq. (A.9) is fulfilled and the Sommerfeld precursor gives an accurate description of the electric field. For the choice $\omega_c = 3.00\times10^{15}$ s$^{-1}$ the inequality on the left-hand-side of Eq. (A.15) gives $\tau < 0.17\epsilon$ fs. With $\gamma = 4\times10^{13}$ s$^{-1}$, $\omega_{pa} = 2.4\times10^{16}$ s$^{-1}$ and $x = 6\times10^{-5}$ m the other inequality gives $\tau < 1.4\cdot10^{-17}\sqrt{\epsilon}$ s. So for $\epsilon = 0.01$ and with oscillation times of $\sim10^{-19}$ s (see Fig. 6) the approximation is accurate over $\sim10^2$ oscillations.

## References


[1] J. Joannopoulos, R. Meade, J. Winn, Photonic Crystals, Molding the Flow of Light, Princeton University Press, 1995.

[2] J. Dowling, C. Bowden, Phys. Rev. A 46 (1992) 612.

[3] J. Munday, M. Robertson, Appl. Phys. Lett. 83 (2003) 1053.

[4] S. Zhu, N. Liu, H. Zheng, H. Chen, Opt. Comm. 174 (2000) 139.

[5] J. Marangos, Nature 397 (1999) 559.

[6] A. Steinberg, P. Kwiat, R. Chiao, Phys. Rev. Lett. 71 (1993) 708.

[7] P. Milloni, J. Phys. B 35 (2002) R31.

[8] M. Mojahedi, E. Schamiloglu, F. Hegeler, K. Malloy, Phys. Rev. E 62 (2000) 5758.

[9] C. Spielmann, R. Szipöcs, A. Stingl, F. Krausz, Phys. Rev. Lett. 73 (1994) 2308.

[10] J. Jackson, Classical Electrodynamics, John Wiley and Sons Inc., 1998.

[11] L. Brillouin, Wave Propagation and Group Velocity, Academic Press Inc., 1960.

[12] K. Oughstun, G. Sherman, Electromagnetic Pulse Propagation in Causal Dielectrics, Springer-Verlag, 1994.

[13] P. Pleshko, I. Palócz, Phys. Rev. Lett. 22 (1969) 1201.

[14] J. Aviksoo, J. Kuhl, K. Ploog, Phys. Rev. A 44 (1991) R5353.

[15] S.-H. Choi, U. Österberg, Phys. Rev. Lett. 92 (2004) 1.

[16] S. Chasteen, http://focus.aps.org/story/v13/st1.

[17] J. Ziman, Principles of the Theory of Solids, Cambridge university press, 1972.

[18] B. Hoenders, M. Bertolotti, J. Opt. Soc. Am. A 22 (2005) 1143.

[19] P. Yeh, A. Yariv, J. Opt. Soc. Am. 67 (1977) 423–438.

[20] P. Yeh, Optical Waves in Layered Media, John Wiley and Sons, 1988.

[21] C. Kittel, Introduction to Solid State Physics, John Wiley and Sons, 1996.

[22] E. Lorch, Spectral Theory, Oxford University Press, 1962.